Pertanika J. Sci. & Technol. 32 (3): 1023 - 1042 (2024)

PERTANIKA JOURNALS

SCIENCE & TECHNOLOGY

Journal homepage: http://www.pertanika.upm.edu.my/

# Anti-friction and Wear Resistance Performance of Palm Olein Grease with Molybdenum Disulfide Additive

**Nadiah Aqilahwati Abdullah, Nurul Farhana Mohd Yusof* and Zaidi Mohd Ripin**

*School of Mechanical Engineering, Engineering Campus, Universiti Sains Malaysia, 14300 Nibong Tebal, Penang, Malaysia*

## ABSTRACT

In this study, palm olein-based grease with a micro-molybdenum disulfide ($MoS_2$) additive has been developed. The grease was prepared using various $MoS_2$ concentrations to investigate the role of additives in improving grease performance. A four-ball tribological test was conducted to investigate the surface morphology, wear depth, and volume loss of the steel ball. The results indicated that the $MoS_2$ additive reduced the coefficient of friction and wear scar diameter compared to pure palm olein grease. The value of 0.5 wt.% was considered the optimum value, reflecting the best grease performance indicated by low friction coefficient, wear diameter, wear depth, and volume loss. Elemental analysis revealed that the $MoS_2$ additive was deposited onto the wear tracks, improving the surface protection. Thus, this additive was found to have a good potential for improving palm olein-based grease.

*Keywords:* Four-ball, friction, $MoS_2$, palm olein grease, wear

ARTICLE INFO

*Article history:*
Received: 14 May 2023
Accepted: 27 November 2023
Published: 01 April 2024

DOI: https://doi.org/10.47836/pjst.32.3.03

*E-mail addresses*:
nadiahaqilah@student.usm.my (Nadiah Aqilahwati Abdullah)
mefarhana@usm.my (Nurul Farhana Mohd Yusof)
mezaidi@usm.my (Zaidi Mohd Ripin)
* Corresponding author

## INTRODUCTION

Lubricants are essential in various industrial applications to minimize friction and wear between the interacting surfaces. In addition, it helps protect metal surfaces from corrosion, operates as a heat transfer fluid, flushes out impurities, absorbs stress, and acts as a seal against dirt, dust, and water. Most commercial greases are based on mineral oil that generally is not environmentally friendly. Mineral oil is not readily biodegradable and is known to pose

ISSN: 0128-7680
e-ISSN: 2231-8526

hazards due to its accumulation in plants, animals, and groundwater (Nowak et al., 2019). It has led the effort to produce a bio-based lubricant with a less toxic base oil. Synthetic oil and vegetable-based oil are the most reliable alternatives to mineral oil as they have desired lubrication properties (Heikal et al., 2017; Hou et al., 2020; Koshy et al., 2015; Quinchia et al., 2014). Synthetic oils offer a wide range of temperature applications and oxidation stability; however, the price is higher than mineral oil.

As a vegetable oil, palm oil possesses excellent properties such as high lubricity, high viscosity index, and low volatility (Yahaya et al., 2018). In addition, palm olein has long fatty acid chains and polar groups that are naturally attracted to metal and provide strong interactions with the lubricated surfaces (Borda et al., 2018; Reeves et al., 2015), which makes it good at boundary lubrication regime (Fox & Stachowiak, 2007; Wang et al., 2022). Palm oil fatty acids consist of unsaturated double bonds, which results in less oxidation stability. Due to this, studies have been conducted by modifying the chemical structure of palm oils. Palm trimethylolpropane ester (TMP) (Gulzar et al., 2017) and double-fractionated palm olein (Zulhanafi & Syahrullail, 2019) are among the modified palm oil derivatives that have been evaluated for their lubrication abilities in the form of lubricating oil. However, major chemical modifications are expensive and tend to reduce the natural tribological properties of vegetable oils.

Palm oil can be further refined as palm olein, which is the liquid fraction of the palm oil after a fractionation process and is in liquid form at room temperature (Pande et al., 2012). The unsaturated fatty acids in the palm olein comprise mono-unsaturated and poly-unsaturated (Yahaya et al., 2018). Despite the unsaturation properties, mono-unsaturated fatty acids have a greater oxidation stability than poly-unsaturated (Fox & Stachowiak, 2007). Palm olein has only 11.0% poly-unsaturated fatty acids, whereas the rest of the compositions come from 50% saturated and 39% mono-unsaturated. In addition, a study proved that palm olein has better oxidation stability at high temperatures than olive oil and rapeseed oil (Tabee et al., 2008). It shows that palm olein can be a good candidate as a lubricant. Palm olein outperformed engine oil without chemical modification in friction reduction properties and exhibited only slightly higher wear scar diameter (Jabal et al., 2014).

In certain applications, grease lubrication is preferable as it requires relatively simple retention devices and is suitable for application under extreme conditions. A thickener must be dispersed in the base oil to develop a grease. It was found that thickeners affect grease's mechanical and thermal stability and play roles in reducing friction and wear (Fan et al., 2018). Despite the existing mineral greases, biological greases derived from vegetable oils have been actively developed as an alternative (Kozdrach & Skowroński, 2018).

A palm bio-grease using calcium soap thickener added with additives (calcium carbonate ($CaCO_3$) and hydroxyapatite (HA)) was produced and investigated for its wear-preventive and extreme pressure properties (Razak & Ahmad, 2021). The study proved that the tribological properties of the formulated bio-based grease are comparable to synthetic-based grease, with great improvement in the load-carrying capacity of the additive-added formulations. In addition, a previous study (Sukirno et al., 2009) produced and evaluated the performance of palm grease using modified refined, bleached, and deodorized (RBD) palm oil and lithium soap thickener. The wear of the palm grease-lubricated specimens was lower than that of the mineral grease-lubricated specimens, indicating good surface protection and anti-wear properties. Thus, adding a thickener can improve the performance of the vegetable oils.

Furthermore, additives are usually added to improve the desired tribological properties of a lubricant. In vegetable grease, copper (Cu) (Borda et al., 2018), molybdenum disulfide ($MoS_2$) (Bagi & Aswath, 2015), and zinc dialkyldithiophosphate (ZDDP) (Nagendramma & Kumar, 2015) are some additives that have been proven to reduce friction and wear. $MoS_2$ particles are among the most common additives due to their layered two-dimensional structure and weak van der Waals force between molecular bonds (Holinski & Gänsheimer, 1972). The effectiveness of $MoS_2$ in enhancing the tribological properties of a lubricant was demonstrated in many studies (Bagi & Aswath, 2015; Gulzar et al., 2015; Koshy et al., 2015). Specifically for vegetable-based oil lubricant, it was reported that 1.0 wt.% $MoS_2$ exhibited good wear protection and high weld load when added to a chemically modified RBD palm oil (Gulzar et al., 2015). In coconut oil, $MoS_2$ nanoparticles produced less friction and wear rate than pure base oil and were accomplished better by adding surfactants (Koshy et al., 2015). Furthermore, the addition of 0.25 wt.% $MoS_2$ nanosheets to white oil demonstrated excellent friction reduction and wear protection compared with the addition of 1.0 wt.% of ZDDP under high load conditions (Wu et al., 2018).

To date, reports on the tribological properties of grease produced from RBD palm oil are very limited (Sukirno et al., 2009, 2010), and the tribological performance of palm grease with RBD palm olein as the base oil has never been reported. Thus, the roles of additives in the RBD palm olein grease remain to be investigated. RBD palm oil is semi-solid at room temperature, consisting of RBD palm olein (liquid fraction) and palm stearin (solid fraction). This study investigates the tribological performance of palm olein-based grease without chemical structure modification of the RBD palm olein base oil to evaluate the effectiveness of thickener and additive ($MoS_2$) on its performance. The micro-scale $MoS_2$ was selected to be used in the study. The selection of the particle sizes was based on a few kinds of literature showing that the effect of $MoS_2$ on the tribological properties is different in different base oils and greases under different testing conditions. For example, (Xu et al., 2013) reported that the micro $MoS_2$ exhibited better lubricating performance than the nano $MoS_2$ when rapeseed oil was used as the base oil. In addition, (Gulzar et al., 2017) tested two sizes of $MoS_2$ in polyalphaolefin (PAO) oil for two different applications. Small-size

(20 nm to 150 nm) particles performed better under the four-ball extreme pressure test, whereas large-size (50 nm to 2000 nm) $MoS_2$ was excellent for cylinder liner application.

In this study, exploring the $MoS_2$ effect on palm grease was initiated using a micro size before going into the nano size in the next stage of the study. A standard four-ball tribometer was utilized to evaluate the tribological properties of the developed greases. Further analysis of the steel ball wear scar is conducted by measuring the wear volume based on the volume of the material loss at the wear scar.

## METHODOLOGY

### Materials

Four samples were prepared in this study: palm oil grease without additive as a reference and another three with different percentages of $MoS_2$ additive. RBD palm olein was purchased from a local distributor, and its properties are presented in Table 1. A lithium 12-hydroxystearate powder was selected as a thickener for the grease formulation. $MoS_2$ with a particle size of 1- 3 µm was used as an additive for this study, as presented in Figure 1. The properties of the $MoS_2$ are listed in Table 1.

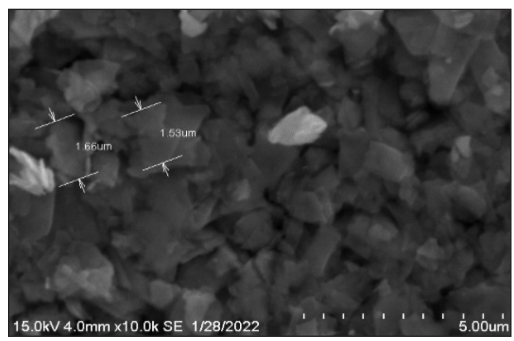


*Figure 1.* Scanning electron microscopy (SEM) image of the $MoS_2$ additive

Table 1
*Properties of the base oil and additive*

| Materials | Properties | |
|---|---|---|
| Base Oil | Density (kg/m$^3$) | 898.2 |
| | Viscosity at 40°C (mm$^2$/s) | 46.76 |
| | Viscosity at 100°C (mm$^2$/s) | 8.91 |
| | Viscosity Index | 174 |
| Thickener | Melting point | 220°C |
| | Color | White |
| Additive | Morphology | Hexagonal with sharp edges |
| | Size | 1-3 µm |
| | Color | Grey |
| | Purity | 98.5% |

### Preparation of the Greases

For grease preparation, 87 wt.% of base oil and 13 wt.% of thickener were added into a glass cylinder on a hot plate and mixed at a temperature of 90°C. Next, the temperature was increased to 160°C while stirring the mixture for 30 min. The temperature was further increased to 210°C while stirring for 5 min and immediately cooled to 120°C to dissolve the lithium. The grease was then separated into four portions for the addition of the additive at different concentrations.

### Dispersion of Additive

The concentration of $MoS_2$ was apportioned into three, specifically 0.25, 0.50, and 0.75

wt.%. The grease temperature was maintained at 120°C while the additive was added to disperse the additive into the grease. An overhead stirrer was used for stirring, and the speed was set to 800 rpm while slowly adding the additive. Once the additive was fully added, the stirrer was sped up to 2200 rpm, and stirring was performed for around 60 min for homogenization.

### Physical Properties of the Grease

The synthesized grease's physical characteristics were assessed using cone penetration and dropping point tests. The cone penetration test followed ASTM D217 guidelines, while the dropping point test adhered to ASTM D556 standards. The resulting measurements for the pure grease indicated a dropping point of 208.7°C and a penetration depth of 276.4 (mm/10), indicating an NLGI 2 grade.

### Friction and Wear Performance

A four-ball tribometer (Ducom TR-30L-IAS, Netherlands) was used to evaluate the friction and wear performance of the greases. The test method was performed in accordance with the Standard Test Method for Wear Preventive Characteristics of Lubricating Grease (ASTM D2266). Figure 2 presents the illustration of the test setup. The experiment was run under a nominal load of 392 N, a rotating speed of 1200 rpm (0.46 m/s), and an operating temperature of 75°C for 60 min. The test used a GCr15 (AISI 52100) steel ball with a 12.7 mm diameter and hardness of 62 to 64 HRC. The initial average surface roughness (Ra) of the ball was measured as 0.1613 µm using Alicona IFM G4. The balls, ball pot set, and chuck were thoroughly cleansed prior to each test using acetone. The wear scar diameter of the balls was measured after each run. Frictional torque obtained from the four-ball torque reading was transformed into the coefficient of friction (COF), and its average value was reported for each sample. New sets of balls were used prior to each test.

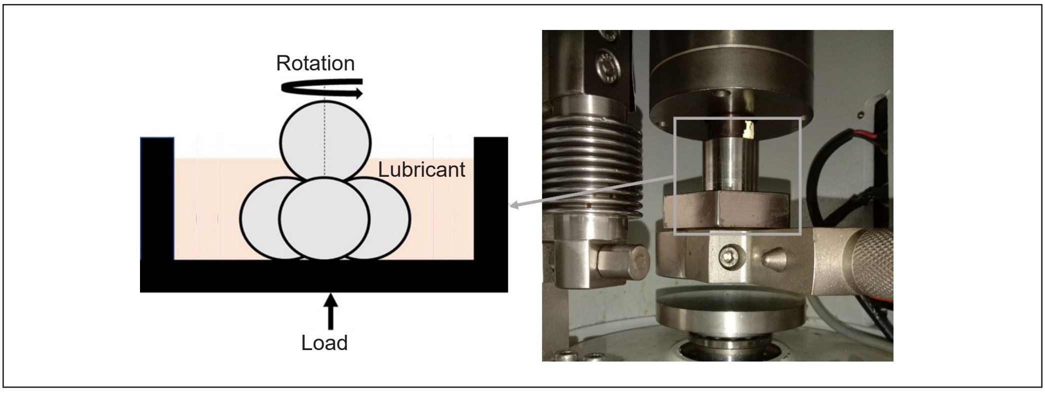


*Figure 2*. Schematic illustration of the DUCOM four-ball test mechanism. The upper ball is rotated at a specified speed while the three lower balls are filled with lubricant

### Analysis of the Worn Surface

A tabletop scanning electron microscopy (Hitachi TM-1000, Japan) with 15 kV accelerating voltage EDX spectroscopy (Oxford Instruments, UK) was adopted to evaluate the characteristics of wear scar surfaces. Each wear scar surface was analyzed at magnifications of 200× and 1200×. Elemental scanning using EDX was made at 1200× magnification. The wear depth profile and volume loss were measured *via* a 3D profilometry (Alicona InfiniteFocus Microscope (IFM) G4, Bruker, USA). Surface scanning was performed on the surface of the steel ball, and the wear depth measurement was performed by obtaining the surface profile perpendicular to the wear grooves. The edge of the wear scar was taken as the reference for the wear depth measurement, as presented in Figure 3(a). The wear volume was obtained by measuring the volume of the material loss at the wear scar area, as presented in Figures 3(b) and 3(c), using the volume measurement feature in the Alicona IFM software. The average roughness (Ra) was measured using the same profilometer for each ball from edge to edge of the wear scar (perpendicular to the wear scratches) with a cutoff length of 0.8 mm.

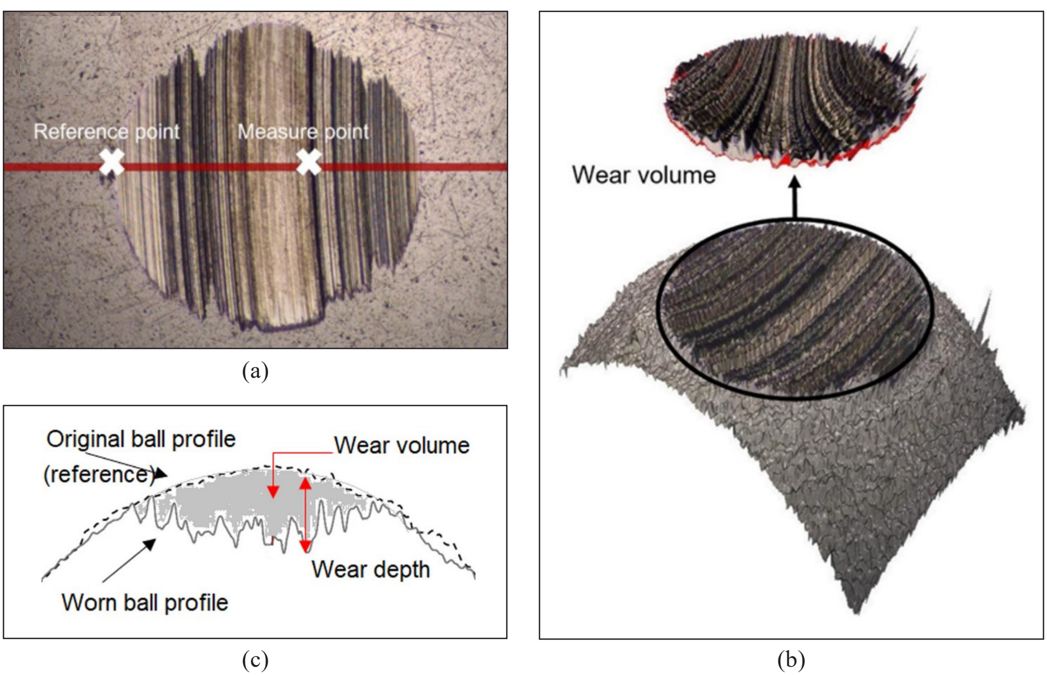


*Figure 3*. Description of the wear depth (a) and wear volume measurement (b and c)

## RESULTS AND DISCUSSION

### COF and Wear Scar Diameter

Figure 4 presents the trend of COF as a function of time for the palm grease with and without additives. The COF values were calculated based on the procedure described in

ASTM D2266. From the graph, the trend is almost identical, where at the first 80 s, the COF exhibits an increasing trend due to a high wear rate where more asperities of the rubbing areas came in contact, leading to plastic deformations of the tips of asperities or known as running-in period (Blau, 2005). Furthermore, the fluctuations of the COF amplitude, especially upon the addition of 0.25 and 0.75 wt.% of $MoS_2$, might be due to the accumulation of wear debris and agglomeration of the additive particles (Nabhan et al., 2021). The COF generally starts to stabilize after 1200 s, where less fluctuation in the amplitude can be observed (Abdollah et al., 2020).

The COF value and wear scar diameter of the greases are presented in Figure 5. It is apparent that the COF value and wear scar diameter decreased with the addition of $MoS_2$. The grease with 0.50 wt.% $MoS_2$ had the lowest COF value of 0.0411 ± 0.0039, followed by 0.25 wt.% $MoS_2$ with a COF value of 0.0421 ± 0.0040, 0.75 wt.% $MoS_2$ with a COF value of 0.0435 ± 0.0045 and pure grease (without additive) with a COF value of 0.0444 ± 0.0043. Under the same tribological test condition (ASTM D2266), the developed pure palm grease had a considerably good friction performance when compared with the friction performance of a mineral grease (COF: 0.089) from a previous study under similar test conditions by He et al. (He et al., 2018), in accordance with the findings from (Abdollah et al., 2020), where palm oil exhibited better friction performance (COF: 0.08) than commercial SAE 15W40 engine oil (COF: 0.12). The excellent performance of the palm oil-

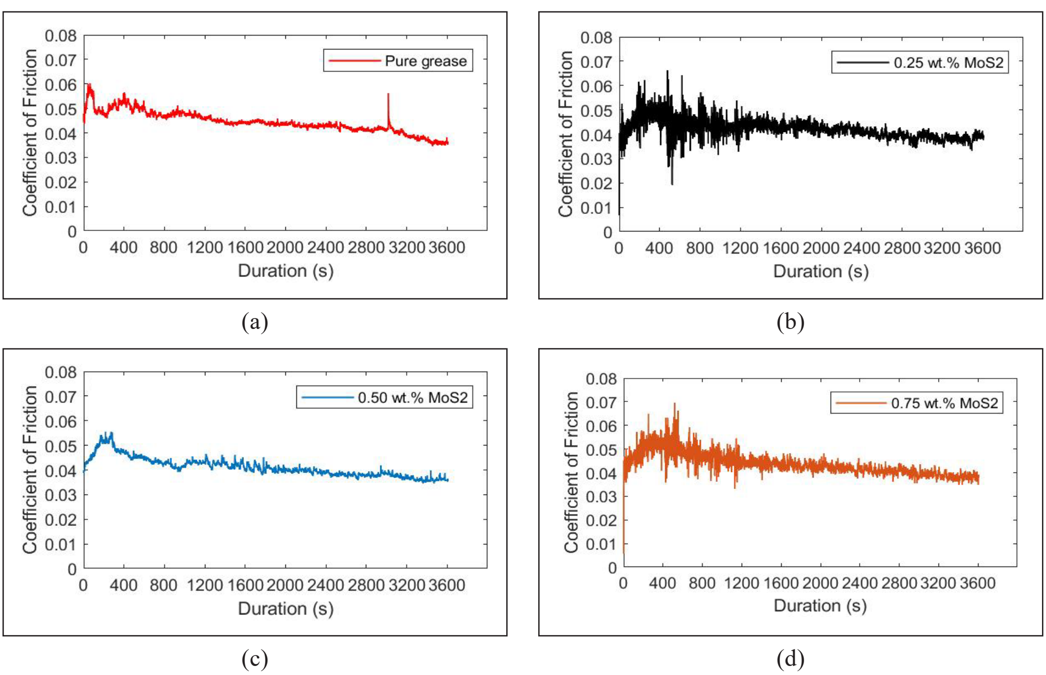


*Figure 4*. Dynamic coefficient of friction: (a) pure palm grease; (b) palm grease + 0.25 wt.% $MoS_2$; (c) palm grease + 0.50 wt.% $MoS_2$; and (d) palm grease + 0.75 wt.% $MoS_2$

based lubricant was due to the base oil polar molecule attraction to the surface material, which reduced the friction (Mannekote & Kailas, 2012; Yahaya et al., 2018).

The relatively good performance of palm olein grease can also be attributed to the synergistic effect between the base oil and the thickener (Fan et al., 2018). In this case, the polarity of the base oil and the thickener can play an important role in their synergistic effect. In the form of oil, the polar heads of the palm fatty acid chains are attached to the metal surface and form a monolayer film with the non-polar end tail of fatty acids facing away from the metal surface (Abdulbari & Zuhan, 2018). In grease, the thickener particles having the same polarity as the palm olein fatty acids will bind together during the grease formulation, allowing the thickener to hold the oil. In addition, palm olein has active sites (unsaturated chains), enabling it to bind with other elements from the thickener and additive while maintaining attraction to the metal surface.

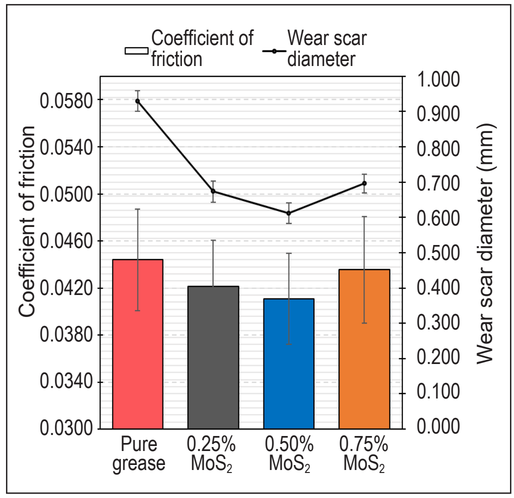

*Figure 5*. Trend of the COF and WSD of the greases

In addition, the physical structure of the palm grease may also contribute to its performance. Palm olein grease can be classified as a viscoelastic material that possesses both elastic and viscous behavior. The elastic part can recoil to its original shape after the stress is removed, whereas the viscous material starts to flow if stress is applied. The elasticity is essential for preventing grease leakage from the lubricated surface. In contrast, fluidity is essential for the grease's lubricating efficiency and to be well dispersed on the rubbing pair.

Furthermore, it was demonstrated that the additive improves the tribological properties of palm-based grease. It was also suggested that the optimum concentration of the $MoS_2$ additive is 0.50 wt.%, which offers the best tribological performance from the wear scar diameter and friction coefficient perspective. Compared with pure grease, the COF was reduced by 7.50%, 5.18%, and 1.92% at the concentrations of 0.50, 0.25, and 0.75 wt.%, respectively. The reduction can be attributed to the additive intrinsic factor, which is a weak van der Waals bond between the molecular layers, where it takes relatively weak shear forces to displace the layers (Holinski & Gänsheimer, 1972). However, the reduction of the COF value was not that significant, which can be explained by the insufficient shearing of $MoS_2$ due to the low load applied (Winer, 1967). In a previous study, Bagi and Aswath (2015) evaluated the performance of $MoS_2$ in lithium grease under different spectrum loading conditions from 40 to 80 kg. They found that higher loads could shear the van der Waals forces between Mo and S better than the lower load, consequently leading to a lower COF value.

In addition, the $MoS_2$ particles in the palm grease might not be able to enter the contact region entirely due to their size. From a previous study by (Hu et al., 2017), micro $MoS_2$ exhibited a lower friction and wear reduction performance compared to nano sizes $MoS_2$, where a nano size is easier to enter the contact region and protect the friction pair. Furthermore, the X-ray photoelectron spectroscopy (XPS) spectra results from the same study showed the occurrence of $MoS_2$ oxidation during the friction process, which leads to the lower particles remaining within the contact region. Therefore, the oxidation of $MoS_2$ might be present, which resulted in the insignificant friction improvement of the palm grease with the addition of micro $MoS_2$.

In the case of different $MoS_2$ concentrations, 0.50 wt.% has better friction performance than 0.25 and 0.75 wt.%. At a concentration of 0.25%, the large wear scar diameter can be attributed to the insufficient amount of MoS, which could not exert a good friction reduction effect compared with the optimum concentration. At $MoS_2$ concentration of 0.75%, the condition can be explained by the possible agglomeration of particles in the palm grease structure. Agglomeration promotes friction due to the increase in shear force required for maintaining the movement between the interacting surfaces whenever the agglomerate particles come into contact (Abdollah et al., 2020; Gong et al., 2021). In other words, agglomeration creates new asperities between the surfaces in contact, which induces high friction and wear to overcome them. Furthermore, agglomeration is closely related to dispersion stability, where a surfactant or dispersant can be introduced into the grease and additive formulation to improve the dispersibility of the additive (Gulzar et al., 2015). However, no surfactant was introduced into the formulation to avoid any influences from the surfactant on the tribological properties of the grease.

The efficiency of a lubricant is determined not only by its ability to provide a low COF but also by its ability to protect a surface from wear. Observation of the wear scar diameter revealed that the grease with 0.50 wt.% $MoS_2$ improved the wear protection with the highest reduction of 31.19% of the scar diameter compared with pure grease, from 0.930 ± 0.029 to 0.612 ± 0.030 mm. $MoS_2$ tends to exhibit a mending effect as one of the lubrication mechanisms where particles are deposited on the wear surface and fill the grooves, which helps reduce the wear (Kumar et al., 2020; Mushtaq & Hanief, 2021). Meanwhile, the diameters of the 0.25 and 0.75 wt.% $MoS_2$ greases have been reduced by 27.63% (to 0.673 ± 0.030 mm) and 25.16% (to 0.696 ± 0.027 mm), respectively. It was observed that 0.25 and 0.75 wt.% $MoS_2$ produced a larger scar diameter than the 0.50 wt. % $MoS_2$. An insufficient amount of additive is expected to result in a slightly larger scar diameter of 0.25 wt.% $MoS_2$ grease. As for the 0.75 wt.% $MoS_2$, a larger scar diameter can be attributed to dispersion stability and particle aggregation along with the sharp edges of the additive, which cause metal rollout and abrasive wear ( Chaurasia et al., 2020).

## Worn Surfaces Morphology

Wear morphology is important in evaluating the wear-protective performance of a lubricant. Scanning electron microscopy (SEM) was employed to characterize the worn surfaces of the steel balls. Figure 6 presents the micrograph image of the wear scar areas on the steel ball after the four-ball test at magnification of 200× and 1200×. A circular scar with deep and shallow parallel grooves was found to form on all worn surfaces. Figure 6(a) presents a worn surface of the ball lubricated with pure grease. The appearance of grooves was more prominent on the pure grease-lubricated surface than on those with additives at 0.25 wt.% $MoS_2$-lubricated surface, noticeable abrasion marks with shallow grooves were observed with a pattern almost similar to pure grease, as presented in Figure 6(b). Figure 6(c) shows that for the 0.50 wt.% $MoS_2$ grease, shallower grooves were formed as a result of the lubrication effect coming from the sufficient additive to fill in the grooves and avoid more severe wear. In addition, the 0.75 wt.% $MoS_2$ produced a wear surface with shallow and deep grooves and visible metal pullout primarily on the focused region, as presented in Figure 6(d). Moreover, sediments were also observed on each surface, deposited onto the surface and filled into scratches.

The sharp edges of $MoS_2$ can cause scratch marks and deep grooves when agglomerate particles are present in the lubricant film. It can be observed at a 1200× magnification scar

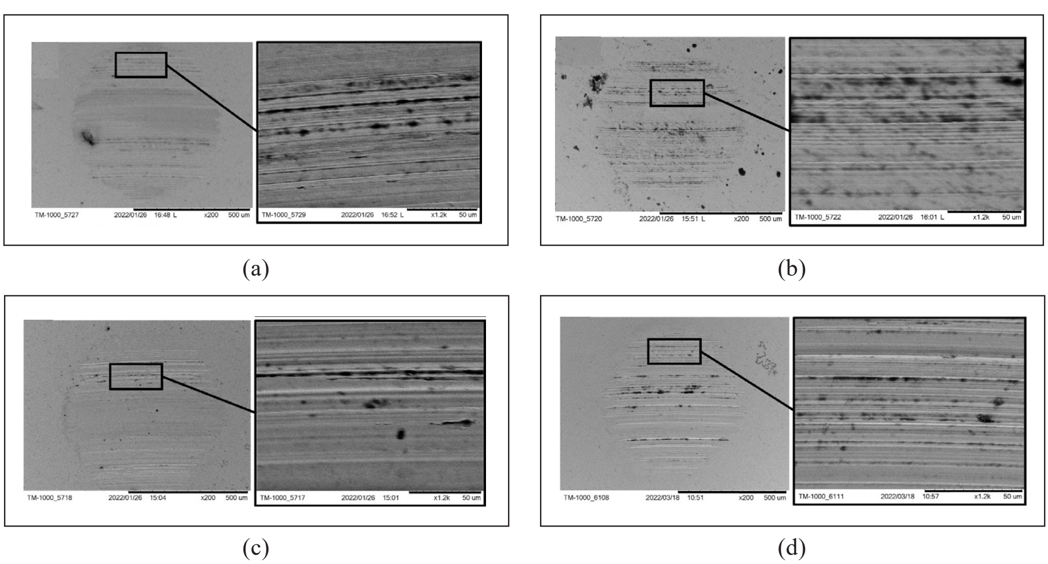


*Figure 6*. SEM images of WSD after the ASTM D2266 tests conducted on (a) pure grease, (b) grease + 0.25 wt.% $MoS_2$, (c) grease + 0.50 wt.% $MoS_2$ and (d) 0.75 wt.% $MoS_2$ at magnifications of 200× (left) and 1200× (right)

image, 0.75 wt.% $MoS_2$ produced ragged edges and deeper grooves than the 0.50 wt.% grease. Abrasive wear was also apparent in the selected region. The additive elements on the worn surface were further validated *via* EDX, measured at a magnification of 1200×.

## Average Roughness of the Wear Region

After the friction and wear test, the average surface roughness (Ra) of the worn steel balls under the grease lubrication was measured *via* 3D profilometry. As can be seen from Figure 8, the average roughness (Ra: 0.7836 ± 0.0900 µm) of the pure grease-lubricated surface [Figure 7 (a)] is lower than those of the other greases. The optimum concentration of $MoS_2$ produced the lowest roughness (Ra: 0.8765 ± 0.0740 µm) among all concentrations, followed by 0.75 wt.% (Ra: 0.8814 ± 0.0431 µm) and 0.25 wt.% (Ra: 1.1063 ± 0.0036 µm). It can be seen that the greases with additives produced higher roughness than the pure grease, which can be attributed to factors such as the shape of the additive particles (Hu, 2005) and the direction of the $MoS_2$ interlayer sliding (Winer, 1967). The orientation of the $MoS_2$ needs to be in the direction of the sliding during the experiment for the interlayer bonded by a weak van der Waals force to be smeared and provide effective film protection (Bagi & Aswath, 2015). As mentioned before, the $MoS_2$ employed in this study has sharp

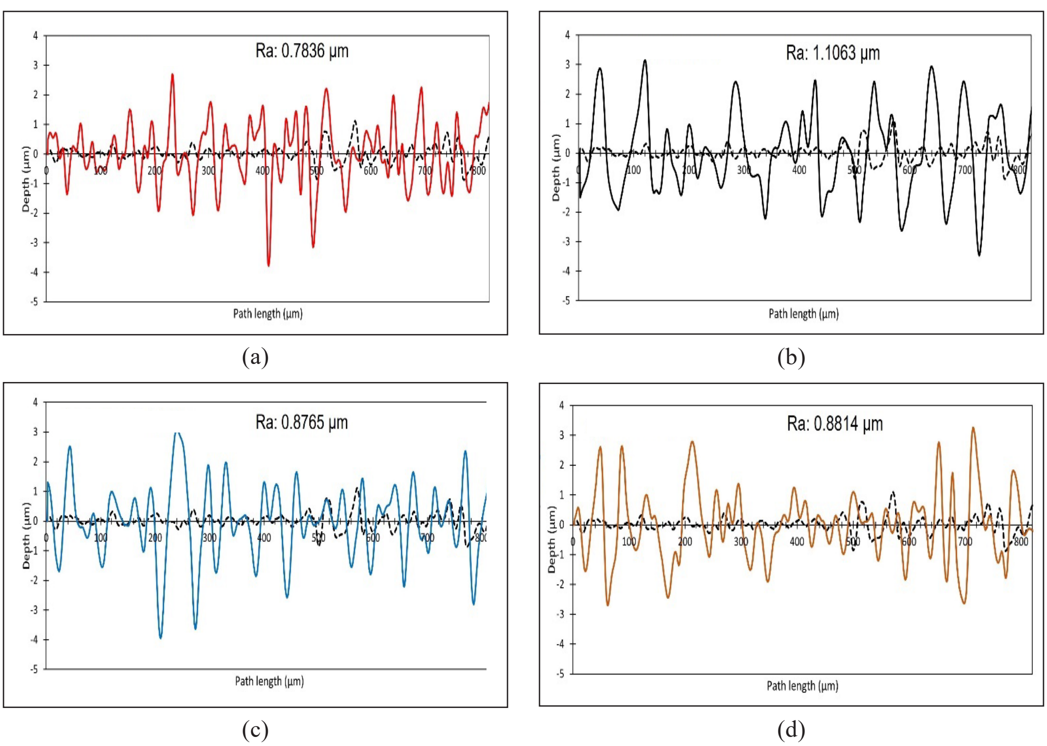


*Figure 7*. Roughness plot: (a) pure grease; (b) 0.25 wt.% $MoS_2$; (c) 0.50 wt.% $MoS_2$; and (d) 0.75 wt.% $MoS_2$. The dotted line plot on every graph indicates the roughness of the ball prior to the test (Ra: 0.1613 µm)

edges, which can cause abrasive wear, especially when the $MoS_2$ is not oriented toward the direction of sliding and particles accumulate during contact (Yu et al., 2019). It is important to note that even though the surface roughness of the grease with $MoS_2$ additive is slightly higher than that of the pure grease, the surface protection in terms of friction and wear is excellent compared with the pure grease.

### Wear Depth Profile and Wear Volume

Further investigation of the wear morphology was performed to quantify the wear depth and volume losses on the steel ball using Alicona IFM—the wear profile of each ball after the experiment is illustrated in Figure 8. The profile shows a significant difference in the scar width between the pure grease and the grease with the $MoS_2$ additive. With the $MoS_2$ additive, the scar diameter becomes smaller with apparent roughness. Figure 9 presents the wear surface topography and wear profile, where the dotted line represents the original shape of the steel ball measured before the experiment. The maximum wear depth for pure grease is high, with a measured value of 35.57 ± 1.12 μm, as presented in Figure 9(a). The presence of $MoS_2$ was found to reduce the wear depth, as presented in Figure 9(b & c); the 0.25 and 0.50 wt.% concentrations reduced the wear depth to 17.92 ± 0.48 and 18.15 ± 0.74 μm, respectively. Figure 9(d) shows that the wear profile becomes rougher, and the wear depth is slightly higher at 19.05 ± 0.81 μm. The finding indicates that the wear depth can be reduced by 48.97% with the optimum additive concentration. The wear depth reduction denotes improved surface protection caused by the deposition of additives on the wear tracks or grooves, which further avoids more severe wear between the contacting surfaces (Qiang et al., 2017).

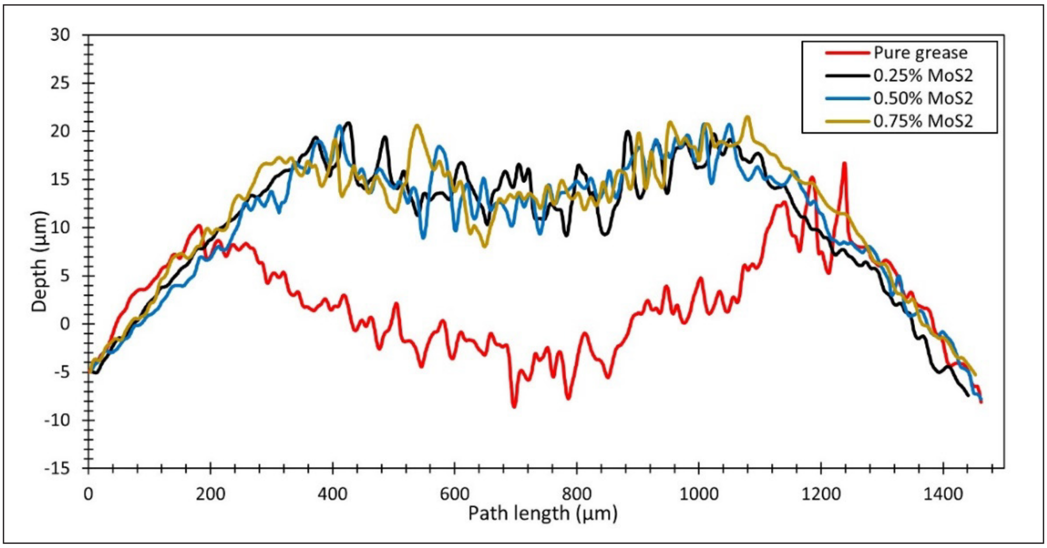


*Figure 8*. The profile of the worn steel balls lubricated with different greases

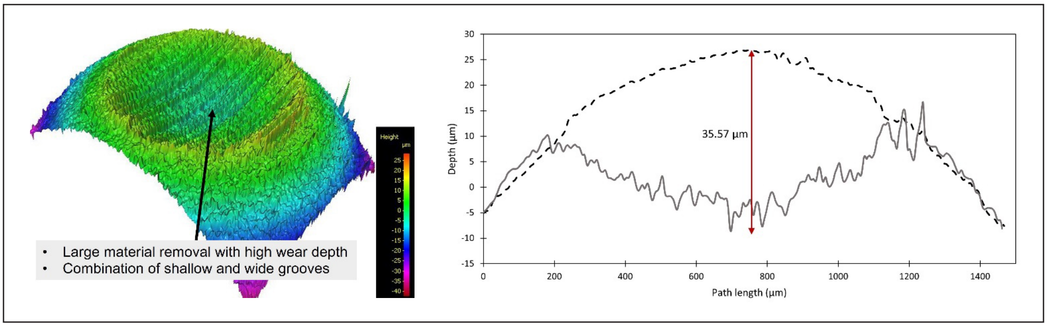


(a)

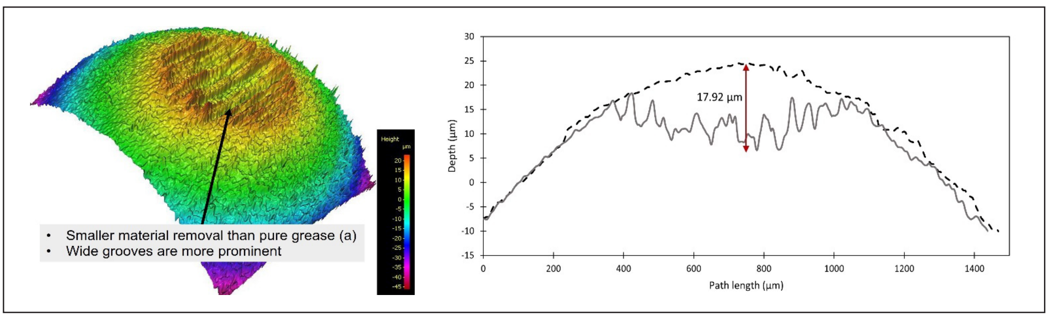


(b)

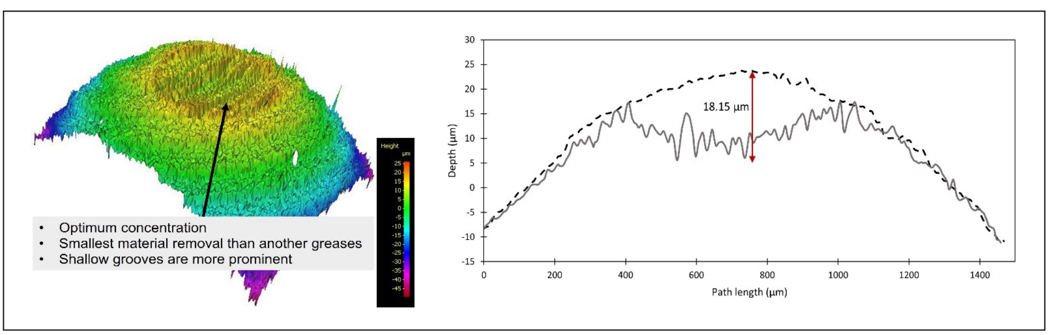


(c)

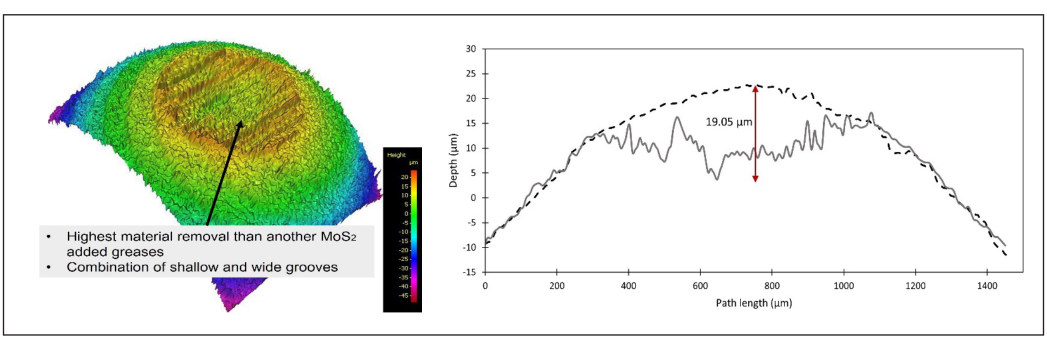


(d)

*Figure 9*. Wear scar morphology and depth of wear of the steel ball lubricated with pure grease (a), grease with 0.25 wt.% $MoS_2$ (b), grease with 0.50 wt.% $MoS_2$ (c), and grease with 0.75 wt.% $MoS_2$ (d)

The wear volume was quantified by measuring the volume of the material removed from the steel ball surface at the wear scar, and the results are presented in Figure 10. Pure grease has a wear volume of around 5.3618 ± 0.1594 × $10^6$ $\mu m^3$. In contrast, the additive significantly reduced the wear volume, where 0.75 wt.% $MoS_2$ produced a wear volume of 1.4385 ± 0.0343 × $10^6$ $\mu m^3$, followed by 0.25 wt.% $MoS_2$ (1.2208 ± 0.1438 × $10^6$ $\mu m^3$), and the lowest, being 0.50 wt.% $MoS_2$ (1.1361 ± 0.0640 × $10^6$ $\mu m^3$). The greases with additives performed better than the pure grease, with 0.50 wt.% $MoS_2$ provides the best wear protection and has the smallest volume of material removed—the 0.25 wt.% $MoS_2$ grease had apparent abrasion marks with larger wear diameter and wear volume compared with the optimum $MoS_2$ grease.

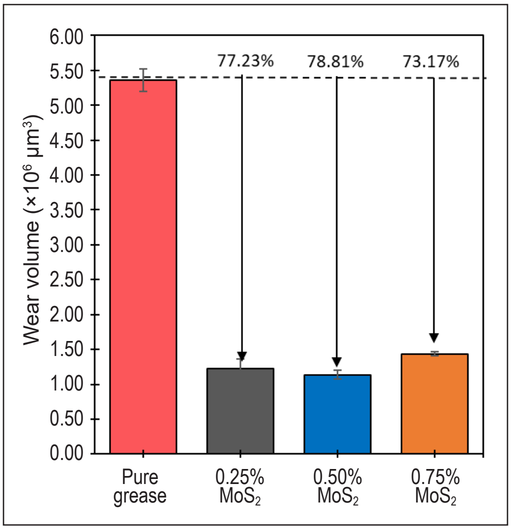


*Figure 10*. Volume loss of the steel balls lubricated with different greases

Moreover, despite having an almost similar wear depth, the 0.75 wt.% $MoS_2$-lubricated surface had a higher wear volume than the 0.50 wt.% $MoS_2$-lubricated surface. From the peak and valley graph of the worn surfaces, it can be seen that the deepest valley of the 0.75 wt.% $MoS_2$-lubricated surface had a width of approximately 60 µm, which can be due to particle agglomeration. Another study has reported the same hypothesis, i.e., agglomerate particles cause deeper abrasive wear and enhanced friction and wear than the optimum additive concentration (Chaurasia et al., 2020).

## Elemental Analysis of the Worn Surfaces

Elemental composition analysis of the wear scar surface was conducted *via* energy-dispersive X-ray spectroscopy (EDX). The related element details of the selected wear scar regions are presented in Figure 11 and Table 2. The Fe, Cr, and C on the worn surface were identified as the main elements of the test steel ball. The deposition of the additive on the wear scar surface can be observed where a molybdenum (Mo) element was detected on the surfaces lubricated with the greases containing an additive, showing that the additive was transferred and accumulated on the surface. Furthermore, Mo existed due to the interlayer shearing of $MoS_2$ and the mending effect where Mo filled the valleys of the wear scratches (Srinivas et al., 2017; Waqas et al., 2021). The 0.75 wt.% $MoS_2$ grease had a higher deposition than the 0.50 wt.% $MoS_2$ grease, indicating that a higher additive concentration induced more deposition on the worn surface. The deposition percentage was similar to

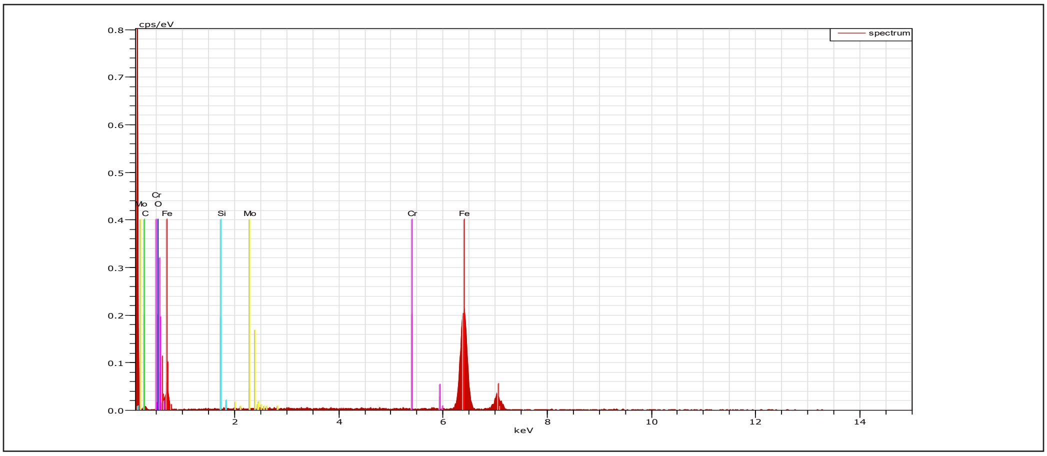


(a)

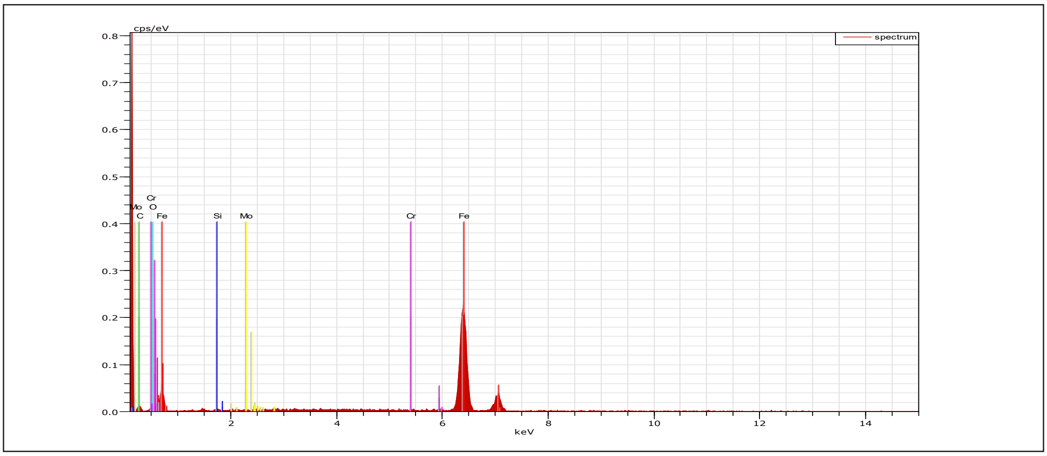


(b)

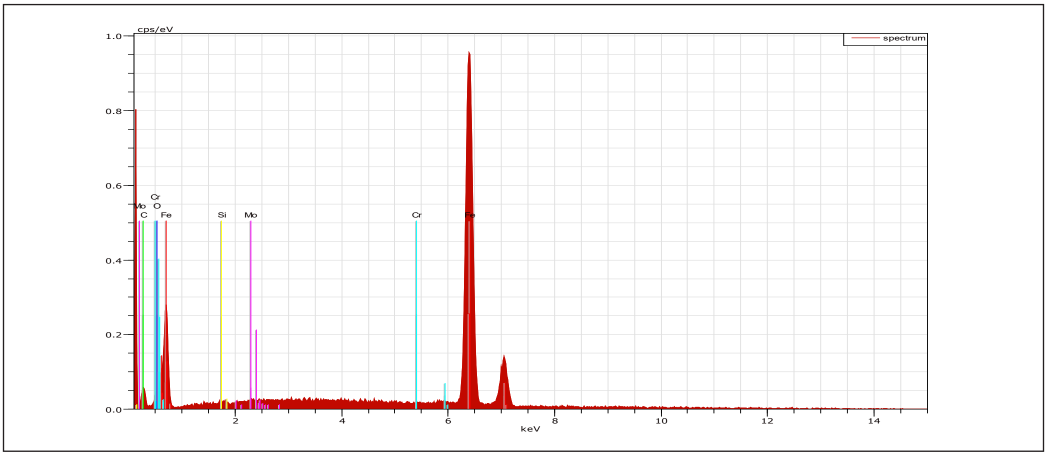


(c)

*Figure 11*. EDX spectra of (a) 0.25 wt.%, (b) 0.50 wt.% and (c) 0.75 wt.% $MoS_2$

that reported in (Wu et al., 2018), where an increase in the $MoS_2$ concentration increased the detected element percentage on the surface. However, the 0.25 wt.% $MoS_2$ yielded a slightly higher Mo percentage than the 0.50 wt.% $MoS_2$. It might be due to more grooves forming on the 0.25 wt.%, providing more space for the $MoS_2$ particles to be deposited (Du et al., 2018).

Table 2
*Elemental composition on the worn surfaces*

| Element | Elemental percentage (wt.%) | | | |
|---|---|---|---|---|
| | Pure Grease | 0.25 wt.% $MoS_2$ | 0.50 wt.% $MoS_2$ | 0.75 wt.% $MoS_2$ |
| C K | 16.35 | 15.33 | 16.55 | 22.19 |
| O K | 0.24 | 0.69 | 1.34 | 1.28 |
| Cr K | 0.39 | 0.55 | 0.36 | 0.34 |
| Fe K | 83.02 | 82.59 | 80.10 | 75.23 |
| Mo L | 0 | 0.83 | 0.74 | 0.96 |

## CONCLUSION

In this study, palm greases have been produced using lithium stearate as a thickener and micro-$MoS_2$ as an additive. Several tests have been conducted to evaluate grease performance, including the tribological test, surface morphology, and wear analysis. From the findings, the following conclusions can be drawn:

- The palm olein grease has a good friction performance and could be enhanced by the presence of a $MoS_2$ additive.
- The $MoS_2$ additive forms a protective layer on the contacting surfaces. The deposition of the additive on the wear scar surface was proven by the detection of the Mo element on the surfaces lubricated with the additive-added greases. This layer efficiently protects the contacting surfaces by reducing friction and wear.
- The value of 0.5 wt.% is the optimum $MoS_2$ concentration, reflecting the best performance of the grease. The lowest friction and wear scar diameters indicate, 0.0411 and 0.612 mm, respectively. Surface morphology analysis also revealed that shallower grooves were formed.
- The ability of the 0.5 wt.% $MoS_2$ to protect the surfaces is indicated by the smallest volume of material removed from the surface with a wear volume of $1.1361 \times 10^6$ $\mu m^3$ and 18.15 μm depth of wear scar.
- The average surface roughness of $MoS_2$-lubricated surfaces was slightly higher than that of pure palm grease. However, among the $MoS_2$ concentrations, the 0.50 wt.% produced the smoothest surface.
- The micro-$MoS_2$ additive has great potential for use as an additive in palm olein-based grease with superior friction and wear performance. The findings also

indicate a good synergistic effect between the palm olein grease and the $MoS_2$ additive, where the combination of both produced better surface protection than palm olein grease alone.

## ACKNOWLEDGEMENTS

The authors express their appreciation to the government of Malaysia under the Ministry of Higher Education for providing research funding through the Fundamental Research Grant Scheme [FRGS/1/2019/TK03/USM/03/4].

## REFERENCES

Abdollah, M. F., Amiruddin, H., & Jamallulil, A. D. (2020). Experimental analysis of tribological performance of palm oil blended with hexagonal boron nitride nanoparticles as an environment-friendly lubricant. *The International Journal of Advanced Manufacturing Technology, 106*, 4183-4191. https://doi.org/10.1007/s00170-019-04906-5

Abdulbari, H. A., & Zuhan, N. (2018). Grease formulation from palm oil industry wastes. *Waste and Biomass Valorization, 9*(12), 2447-2457. https://doi.org/10.1007/s12649-018-0237-6

American Society for Testing and Materials. (2017). *Standard test methods for cone penetration of lubricating grease (ASTM D217-02).* ASTM International.

American Society for Testing and Materials. (2010). *Standard test method for dropping point of lubricating grease (ASTM D556-02).* ASTM International.

American Society for Testing and Materials. (2010). *Standard test method for wear preventive characteristics of lubricating grease (Four-ball method) (ASTM D 2266 – 01).* ASTM International

Bagi, S. D., & Aswath, P. B. (2015). Mechanism of friction and wear in $MoS_2$ and ZDDP/F-PTFE greases under spectrum loading conditions. *Lubricants, 3*(4), 687-711. https://doi.org/10.3390/lubricants3040687

Blau, P. (2005). On the nature of running-in. *Tribology International, 38*(11-12), 1007-1012. https://doi.org/10.1016/j.triboint.2005.07.020

Borda, F. L. G., Oliveira, S. J. R., Lazaro, L. M. S. M., & Leiroz, A. J. K. (2018). Experimental investigation of the tribological behavior of lubricants with additive containing copper nanoparticles. *Tribology International, 117*, 52-58. https://doi.org/10.1016/j.triboint.2017.08.012

Chaurasia, S. K., Singh, N. K., & Singh, L. K. (2020). Friction and wear behavior of chemically modified Sal (*Shorea Robusta*) oil for bio based lubricant application with effect of CuO nanoparticles. *Fuel, 282*, Article 118762. https://doi.org/10.1016/j.fuel.2020.118762

Du, S., Sun, J., & Wu, P. (2018). Preparation, characterization and lubrication performances of graphene oxide-$TiO_2$ nanofluid in rolling strips. *Carbon, 140*, 338-351. https://doi.org/10.1016/j.carbon.2018.08.055

Fan, X., Li, W., Li, H., Zhu, M., Xia, Y., & Wang, J. (2018). Probing the effect of thickener on tribological properties of lubricating greases. *Tribology International, 118*, 128-139. https://doi.org/10.1016/j.triboint.2017.09.025

Fox, N. J., & Stachowiak, G. W. (2007). Vegetable oil-based lubricants - A review of oxidation. *Tribology International, 40*(7), 1035-1046. https://doi.org/10.1016/j.triboint.2006.10.001

Gong, L., Qian, S., Wang, W., Ni, Z., & Tang, L. (2021). Influence of nano-additives (nano-PTFE and nano-$CaCO_3$) on tribological properties of food-grade aluminum-based grease. *Tribology International, 160*, Article 107014. https://doi.org/10.1016/j.triboint.2021.107014

Gulzar, M., Mahmood, K., Zahid, R., Alabdulkarem, A., Masjuki, H. H., Kalam, M. A., Varman, M., Zulkifli, N. W. M., Ahmad, P., & Malik, M. S. S. (2017). The effect of particle size on the dispersion and wear protection ability of $MoS_2$ particles in polyalphaolefin and trimethylolpropane ester. *Proceedings of the Institution of Mechanical Engineers, Part J: Journal of Engineering Tribology, 232*(8), 987-998. https://doi.org/10.1177/1350650117749404

Gulzar, M., Masjuki, H. H., Varman, M., Kalam, M. A., Mufti, R., Mohd Zulkifli, N. W., Yunus, R., & Zahid, R. (2015). Improving the AW/EP ability of chemically modified palm oil by adding CuO and $MoS_2$ nanoparticles. *Tribology International, 88*, 271-279. https://doi.org/10.1016/j.triboint.2015.03.035

He, Q., Li, A., Guo, Y., Liu, S., Zhang, Y., & Kong, L. (2018). Tribological properties of nanometer cerium oxide as additives in lithium grease. *Journal of Rare Earths, 36*(2), 209-214. https://doi.org/10.1016/j.jre.2017.09.004

Heikal, E. K., Elmelawy, M. S., Khalil, S. A., & Elbasuny, N. M. (2017). Manufacturing of environment friendly biolubricants from vegetable oils. *Egyptian Journal of Petroleum, 26*(1), 53-59. https://doi.org/10.1016/j.ejpe.2016.03.003

Holinski, R., & Gänsheimer, J. (1972). A study of the lubricating mechanism of molybdenum disulfide. *Wear, 19*(3), 329-342. https://doi.org/10.1016/0043-1648(72)90124-X

Hou, X., Jiang, H., Ali, M. K. A., Liu, H., Su, D., & Tian, Z. (2020). Dispersion behavior assessment of the molybdenum disulfide nanomaterials dispersed into poly alpha olefin. *Journal of Molecular Liquids, 311*, Article 113303. https://doi.org/10.1016/j.molliq.2020.113303

Hu, E. Z., Xu, Y., Hu, K. H., & Hu, X. G. (2017). Tribological properties of 3 types of $MoS_2$ additives in different base greases. *Lubrication Science, 29*(8), 541-555. https://doi.org/10.1002/ls.1387

Hu, X. (2005). On the size effect of molybdenum disulfide particles on tribological performance. *Industrial Lubrication and Tribology, 57*(6), 255-259. https://doi.org/10.1108/00368790510622353

Jabal, M. H., Ani, F. N., & Syahrullail, S. (2014). The tribological characteristic of the blends of RBD palm olein with mineral oil using four-ball tribotester. *Jurnal Teknologi, 69*(6), 11-14. https://doi.org/10.11113/jt.v69.3232

Koshy, C. P., Rajendrakumar, P. K., & Thottackkad, M. V. (2015). Evaluation of the tribological and thermo-physical properties of coconut oil added with $MoS_2$ nanoparticles at elevated temperatures. *Wear, 330-331*, 288-308. https://doi.org/10.1016/j.wear.2014.12.044

Kozdrach, R., & Skowroński, J. (2018). The application of polyvinylpyrrolidone as a modifier of tribological properties of lubricating greases based on linseed oil. *Journal of Tribology, 140*(6), Article 061801. https://doi.org/10.1115/1.4040054

Kumar, N., Saini, V., & Bijwe, J. (2020). Performance properties of lithium greases with PTFE particles as additive: Controlling parameter-size or shape? *Tribology International, 148*, Article 106302. https://doi.org/10.1016/j.triboint.2020.106302

Mannekote, J. K., & Kailas, S. V. (2012). The effect of oxidation on the tribological performance of few vegetable oils. *Journal of Materials Research and Technology, 1*(2), 91-95. https://doi.org/10.1016/S2238-7854(12)70017-0

Mushtaq, Z., & Hanief, M. (2021). Evaluation of tribological performance of jatropha oil modified with molybdenum disulphide micro-particles for steel-steel contacts. *Journal of Tribology, 143*(2), Article 021401. https://doi.org/10.1115/1.4047752

Nabhan, A., Rashed, A., Ghazaly, N. M., Abdo, J., & Haneef, M. D. (2021). Tribological properties of $Al_2O_3$ nanoparticles as lithium grease additives. *Lubricants, 9*(1), Article 9. https://doi.org/10.3390/lubricants9010009

Nagendramma, P., & Kumar, P. (2015). Eco-friendly multipurpose lubricating greases from vegetable residual oils. *Lubricants, 3*(4), 628-636. https://doi.org/10.3390/lubricants3040628

Nowak, P., Kucharska, K., & Kamiński, M. (2019). Ecological and health effects of lubricant oils emitted into the environment. *International Journal of Environmental Research and Public Health, 16*(16), Article 3002. https://doi.org/10.3390/ijerph16163002

Pande, G., Akoh, C. C., & Lai, O. M. (2012). 19 - Food uses of palm oil and its components. In O. M. Lai, C. P. Tan & C. C. Akoh (Eds.), *Palm Oil* (pp. 561-586). AOCS Press. https://doi.org/10.1016/B978-0-9818936-9-3.50022-8

Qiang, H., Anling, L., Yangming, Z., Liu, S., & Yachen, G. (2017). Experimental study of tribological properties of lithium-based grease with Cu nanoparticle additive. *Tribology-Materials, Surfaces & Interfaces, 11*(2), 75-82. https://doi.org/10.1080/17515831.2017.1311560

Quinchia, L. A., Delgado, M. A., Reddyhoff, T., Gallegos, C., & Spikes, H. A. (2014). Tribological studies of potential vegetable oil-based lubricants containing environmentally friendly viscosity modifiers. *Tribology International, 69*, 110-117. https://doi.org/10.1016/j.triboint.2013.08.016

Razak, I. H. A., & Ahmad, M. A. (2021). Tribological behavior of calcium complex palm-biogrease with green additives. *Tribology in Industry, 43*(1), 139-149. https://doi.org/10.24874/ti.1002.11.20.02

Reeves, C. J., Menezes, P. L., Jen, T. C., & Lovell, M. R. (2015). The influence of fatty acids on tribological and thermal properties of natural oils as sustainable biolubricants. *Tribology International, 90*, 123-134. https://doi.org/10.1016/j.triboint.2015.04.021

Srinivas, V., Thakur, R. N., Jain, A. K., & Babu, M. S. (2017). Tribological studies of transmission oil dispersed with molybdenum disulfide and tungsten disulfide nanoparticles. *Journal of Tribology, 139*(4), Article 041301. https://doi.org/10.1115/1.4034766

Sukirno, Fajar, R., Bismo, S., & Nasikin, M. (2009). Biogrease based on palm oil and lithium soap thickener: Evaluation of antiwear property. *World Applied Sciences Journal, 6*(30), 401-407.

Sukirno, Ludi, Fajar, R., Bismo, & Nasikin. (2010). Anti-wear properties of bio-grease from modified palm oil and calcium soap thickener. *Agricultural Engineering International: The CIGR Journal, 12*(2), 64-69.

Tabee, E., Azadmard-Damirchi, S., Jägerstad, M., & Dutta, P. C. (2008). Effects of α-tocopherol on oxidative stability and phytosterol oxidation during heating in some regular and high-oleic vegetable oils. *Journal of the American Oil Chemists' Society, 85*(9), 857-867. https://doi.org/10.1007/s11746-008-1274-2

Wang, W., Zhao, W., Ma, Q., Kouediatouka, A. N., Zhang, H., Dong, G., Hua, M., & Tam, H. Y. (2022). Synergistic lubrication for textured surfaces using polar and nonpolar lubricants. *Journal of Tribology, 145*(1), Article 012201. https://doi.org/10.1115/1.4055715

Waqas, M., Zahid, R., Bhutta, M. U., Khan, Z. A., & Saeed, A. (2021). A review of friction performance of lubricants with nano additives. *Materials, 14*(21), Article 6310. https://doi.org/10.3390/ma14216310

Winer, W. O. (1967). Molybdenum disulfide as a lubricant: A review of the fundamental knowledge. *Wear, 10*(6), 422-452. https://doi.org/10.1016/0043-1648(67)90187-1

Wu, H., Wang, L., Johnson, B., Yang, S., Zhang, J., & Dong, G. (2018). Investigation on the lubrication advantages of $MoS_2$ nanosheets compared with ZDDP using block-on-ring tests. *Wear, 394-395*, 40-49. https://doi.org/10.1016/j.wear.2017.10.003

Xu, Z. Y., Hu, K. H., Han, C. L., Hu, X. G., & Xu, Y. F. (2013). Morphological influence of molybdenum disulfide on the tribological properties of rapeseed oil. *Tribology Letters, 49*(3), 513-524. https://doi.org/10.1007/s11249-012-0092-8

Yahaya, W. M. A. W., Dandan, M. A., Samion, S., & Musa, M. N. (2018). A comprehensive review on palm oil and the challenges using vegetable oil as lubricant base-stock. *Journal of Advanced Research in Fluid Mechanics and Thermal Sciences, 52*(2), 182-197.

Yu, R., Liu, J., & Zhou, Y. (2019). Experimental study on tribological property of $MoS_2$ nanoparticle in castor oil. *Journal of Tribology, 141*(10), Article 102001. https://doi.org/10.1115/1.4044294

Zulhanafi, P., & Syahrullail, S. (2019). The tribological performances of super olein as fluid lubricant using four-ball tribotester. *Tribology International, 130*, 85-93. https://doi.org/10.1016/j.triboint.2018.09.013